SIEMENS
Ingenuity for life

Validating Simcenter STAR-CCM+ In-cylinder solution

Siemens and Daimler AG research on simulation of gas exchange

Executive summary

Capturing global in-cylinder quantities and details of the turbulent flow characteristics at a high level of accuracy is a precondition to any sophisticated in-cylinder simulation like mixture preparation and combustion prediction. Together with Siemens, the research department of Daimler AG conducted a study on transient Reynolds-averaged Navier-Stokes (RANS) simulation of gas exchange in an optically accessible gasoline direct injection engine to assess the capabilities of the Simcenter™ STAR-CCM+™ In-cylinder solution.

siemens.com/simcenter

Contents

Introduction

CFD simulation of internal combustion engines has reached a high level of complexity over the past decades.[1] Available in-cylinder models cover the process from turbulent gas exchange, spray injection, fuel evaporation and mixing, combustion to knock and emissions formation.[2,3,4] However, analyzing this process chain from its very end, it becomes obvious how sensitive it is to first principles: emission reactions rates are tied to temperature; temperature is a consequence and dominating factor of heat release from combustion. Combustion and emissions are a function of scalar concentrations and turbulent scales. Scalar concentration is dominated by spray evaporation, convection and (turbulent) diffusion. Spray dynamics is affected by the velocity field and turbulent dispersion. Turbulent length and time scales result from turbulent kinetic energy and dissipation rate. Finally, all the above are tied to the velocity field and its gradients. In short, the fidelity of predicting the chain of physics in the combustion chamber is fundamentally relying on the prediction of the turbulent velocity field with a significant level of sensitivity.[6,7]

Objectives of the study
This work presents the simulation of the gas exchange in an optical accessible gasoline direct injection engine in motored conditions using the In-cylinder solution add-on to Simcenter STAR-CCM+ software. A major goal is to verify that Simcenter STAR-CCM+ captures all relevant flow features and cylinder bulk quantities with a high level of accuracy. Validation is done against high-speed dual-plane PIV experimental data and results are compared to a STAR-CD™ software reference simulation, both available from previous works.[1] Cycle-to-cycle convergence and mesh sensitivity of the CFD solution are analyzed.

A major goal of the study was to verify simulation capabilities for complex internal combustion engine flows in a RANS formulation. Results are validated against high-speed, two-component, two-dimensional, dual-plane particle image velocimetry (PIV) measurements carried out simultaneously in the central tumble and mid-intake valve plane under motored conditions. Furthermore, results are compared with a validated STAR-CD reference solution stemming from previous works. The study includes the assessment of cycle-to-cycle convergence of integrated averaged flow values (trapped mass, tumble,

turbulent kinetic energy), as well as of the space and time resolved velocity field. It proves that cyclic convergence, characteristic to RANS ensemble average, is reached after a maximum of three cycles where second cycle results already within a 5 percent range of the reference converged cycle solution. In a high level of detail, relevant flow field features are captured by Simcenter STAR-CCM+ in comparison to PIV measurements. A mesh sensitivity analysis reveals that solution dependency becomes insignificant below 0.75 mm cell base size. An assessment of turbulent model sensitivity shows its crucial importance to consistency between STAR-CD and Simcenter STAR-CCM+ results.

Research engine configuration
The study has been carried out on a single-cylinder gasoline direct injection (GDI) research engine with optical access. The geometry is derived from a current Daimler 2.0 L gasoline 4-cylinder, 4-stroke engine and can be regarded as representative of a state-of-the-art spray-guided, spark-ignited GDI engine.[8] It features a deeply-penetrating spark-plug, central injector location and close-to-series intake and exhaust ports, piston shape and cylinder head.

An overview of the major engine data can be found in Table 1.

Table 1 – Engine data

Bore	83 mm
Stroke	92 mm
Compression ratio	9.5
Engine speed	2,000 RPM
Engine load	motored
Intake valve opening	366 ° CA
Intake valve closing	594 ° CA

With 2,000 RPM the revolution speed is comparably high for optical accessible research engines, yielding realistic conditions to assess the applicability of the CFD methodology to production engine development.
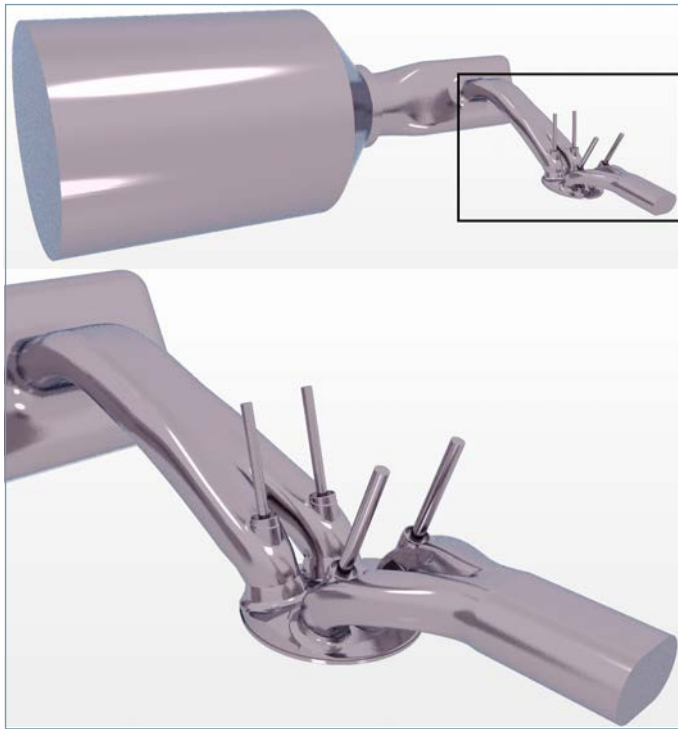
Figure 1: Engine geometry (bottom) and complete CFD domain (top).

Particle image velocimetry measurements

All measurements were carried out at the Daimler AG research and development department. The employment of two independent PIV measurement devices allows for time-resolved two-dimensional, two-component PIV measurements. This yields quasi-simultaneous information on the flow field in the central tumble plane and mid intake valve plane at a high sampling rate.

Simulation details

Apart from STAR-CD reference results, all simulations were carried out using the first release of the Simcenter STAR-CCM+ In-cylinder solution (Simcenter STAR-CCM+ version 12.06). The simulation domain includes the airbox, ports and cylinder volume (figure 1). The analysis is performed under motored conditions with according transient pressure and temperature boundaries and moderate wall temperatures. Physical models and numerics are based on default settings, reflecting best practices. This includes realizable k-epsilon turbulence model with two-layer, all y+ wall treatment, implicit unsteady solver with second-order discretization and a time step of 1.0E-5 seconds with automatic reduction during low valve lift periods. Valve gap distance at which a disconnection between cyclinder and ports is enforced is 0.1 mm. Mesh generation is based on a fully
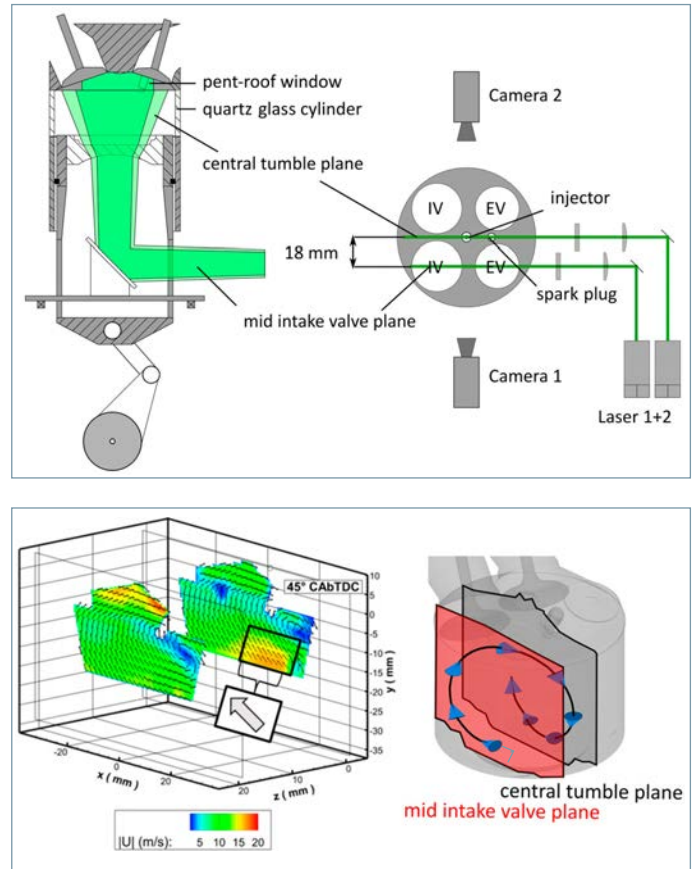

Figure 2: Dual PIV measurement system.

automated process using Simcenter STAR-CCM+ In-cylinder solution: trimmed meshes are morphed with piston and valve motion and automatically remeshed on-the-fly as cell distortion requires. Major baseline mesh specifications are summarized in Table 2.

Table 2 – Mesh characteristics

Mesh type	Trimmed
Mesh motion	Morph/ remesh/ map solution
Volume cell base size	0.75 mm
Prism layer thickness	0.4 mm
Number of prism layers	2
Prism thickness ratio	1

Local embedded refinements are automatically created around valves and in the crevice region. Moreover, user-defined refinements were added near the spark plug and injector. The airbox and intake manifold mesh was added to the simulation as a polyhedral mesh.

Results

Integrated cylinder quantities

Figure 3 proves an excellent cycle-by-cycle convergence of the Simcenter STAR-CCM+ solution after two to three consecutive cycles. As the graphs prove, the RANS-based simulation yields a cyclic repetitive pressure trace for both the intake port and the combustion chamber after effects of the initialization vanish with the second cycle.
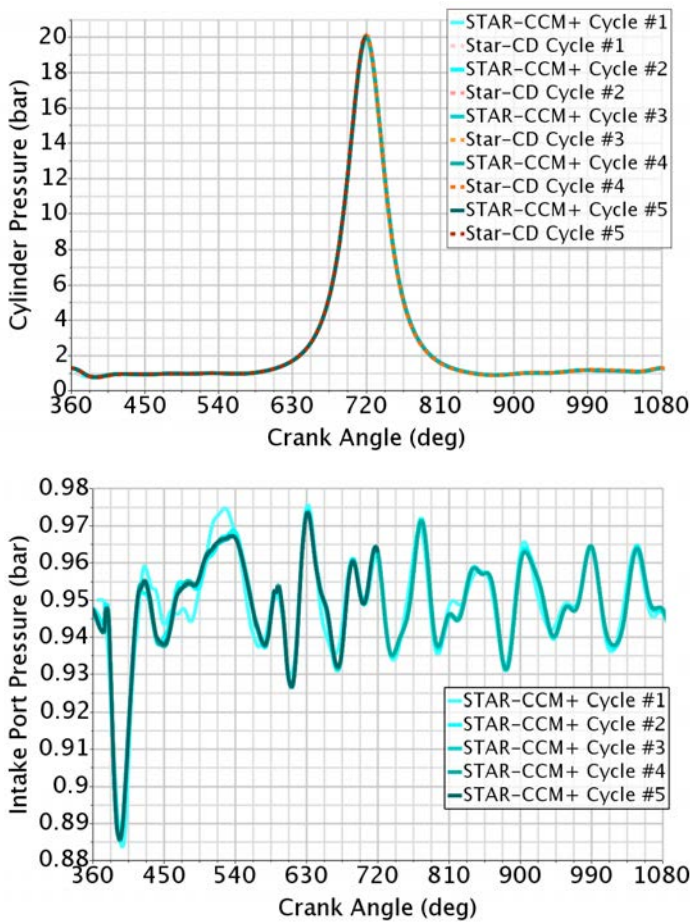
A similar behavior is observed for the cylinder (trapped) mass evolution; see figure 4. Furthermore, the graphs prove a very similar quantitative prediction of cylinder mass evolution between STAR-CD, Siemens' legacy in-cylinder solution and the new Simcenter STAR-CCM+ In-cylinder solution for the five cycles simulated.
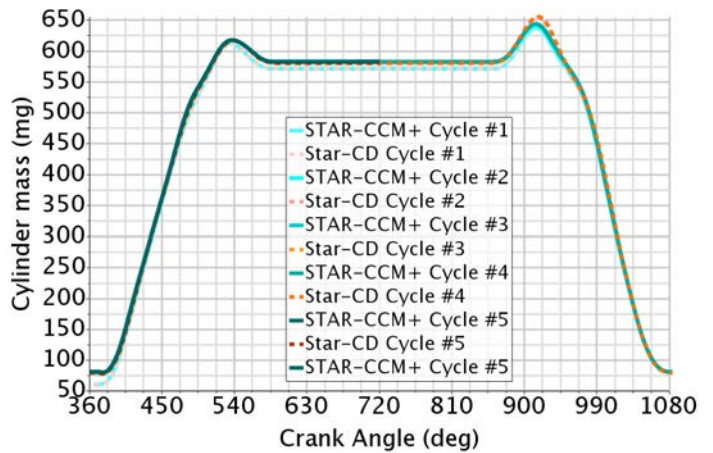

Figure 4: Cylinder mass evolution.

Focusing on the bulk motion properties, STAR-CD and Simcenter STAR-CCM+ show the typical transient tumble evolution.[9,10,11] While again tumble is very similar for both codes during downstroke, it shows notable differences in late upstroke tumble evolution.

Figure 3: Transient evolution of the in-cylinder (top) and intake port (bottom) pressure overlaid for five consecutive cycles.
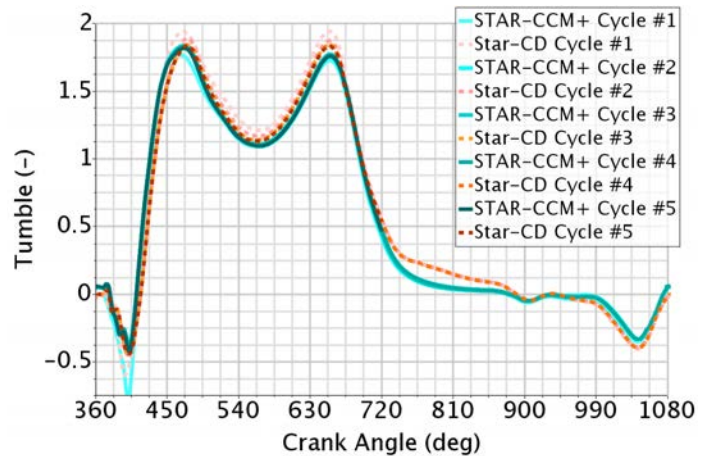

Figure 5: y-tumble evolution.

Likewise, differences can be obtained between the codes in turbulent kinetic energy (TKE) levels, especially approaching TDC; see figure 6.
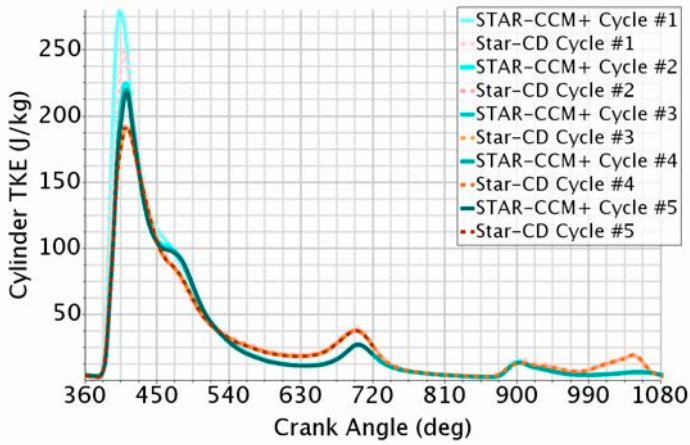

Figure 6: Turbulent kinetic energy evolution.

While the absolute validity of one or the other TKE results cannot be judged due to the lack of experimental evidence, an assessment of the two tumble evolutions can be based on PIV measurements; see next section.

As can be seen from figure 7, Simcenter STAR-CCM+, like STAR-CD, in general reaches a converged cyclic state within a five percent limit from the reference solution (cycle 5) for all relevant cylinder bulk properties within only two cycles with no relevant cyclic fluctuations in the RANS solution thereafter.

Like for cylinder-averaged quantities, appendix B proves that the velocity field and local characteristic flow features do not change after the second cycle. This is a clear indication of the high-accuracy RANS ensemble-averaging capabilities of both CFD solvers. It is a crucial detail for repeatable, consistent and effective assessment of the average engine cycle.
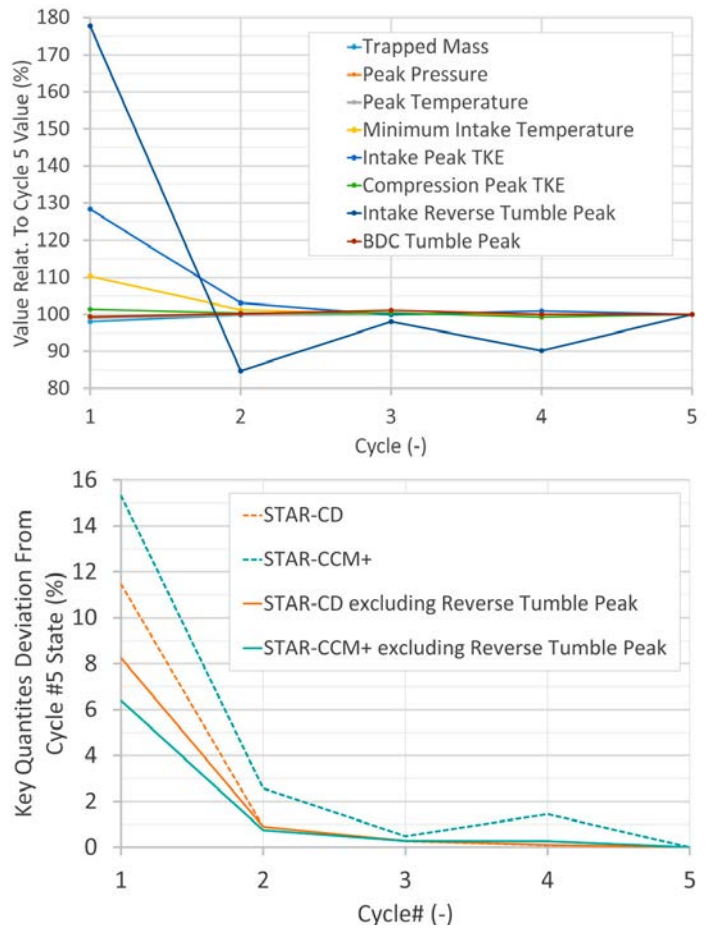

Figure 7: Cycle-to-cycle convergence of major in-cylinder metrics in Simcenter STAR-CCM+, (individually – top; combined average – bottom).

High-speed PIV comparison

According to previous works the engine flow is characterized by four main dominant flow structures; see figure 8. As structures 1 and 3 have similar strength and interact at the exhaust side due to the specific engine design at hand, corresponding impinging turbulent jet flows are inherently unstable and therefore a challenge to the RANS CFD.
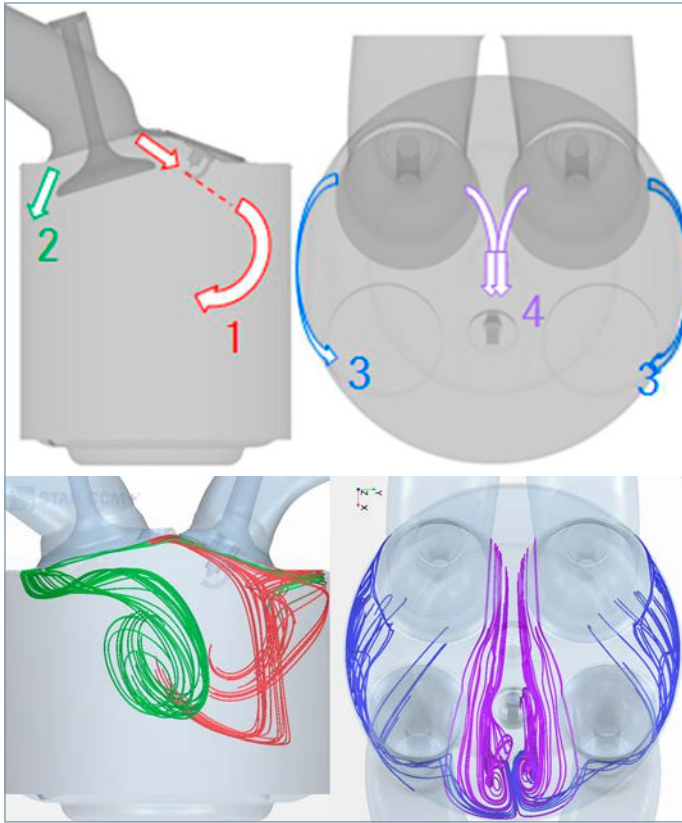

Figure 8: Main flow structures schematic/expected (top) and predicted by CFD /streamlines (bottom); tumble flow (red), filling flow (green), side flow (blue), central flow (purple).

Appendix A shows a comparison of the PIV measurements with the Simcenter STAR-CCM+ and STAR-CD velocity field in the central tumble plane during the cycle. It reveals that all relevant major flow structures are captured by CFD with high accuracy: during intake the obstructing effect of the deeply penetrating spark plug on the intake air jet (1) becomes noticeable; appendix A, 450° crank angle (CA). While the main jet evolves the central plane velocity field becomes affected by the side flow (3) entering the central tumble plane, figure 9.
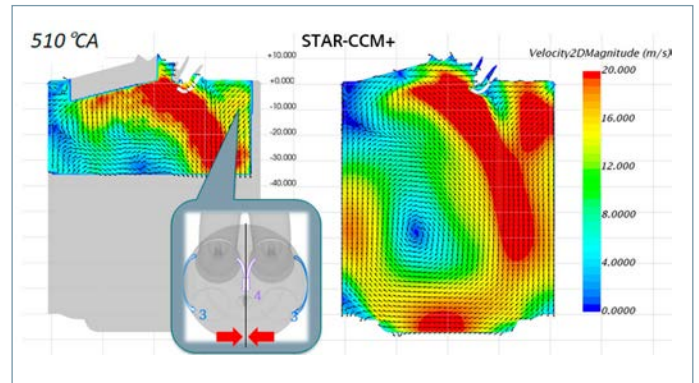

Figure 9: Secondary flow structure resulting from side flows impinging in the central plane between the exhaust valves, PIV (left) and Simcenter STAR-CCM+ simulation (right).

Even though slightly overestimated in its strength by the RANS CFD it is crucial that the simulation is able to capture this detail.

As the piston passes through bottom dead center (BDC) and the tumble is fully evolved, timing, location and strength of the main tumble upwards flow during compression is excellently predicted; figure 10 and appendix A.
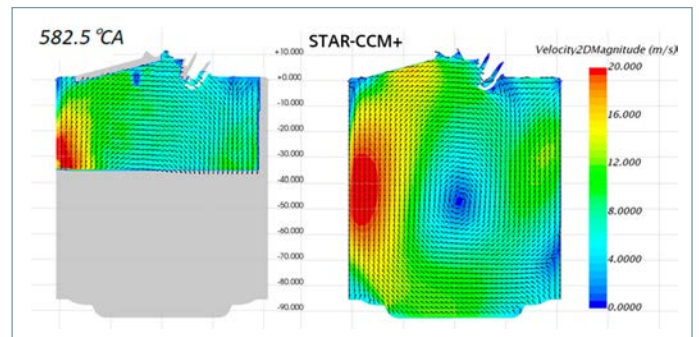

Figure 10: Upward tumble flow, PIV (left) and Simcenter STAR-CCM+ simulation (right).

Again, the latter is well predicted by the CFD in both strength and location. Figure 11 shows the tumble center trajectories for Simcenter STAR-CCM+, STAR-CD and PIV proving that STAR-CCM+ was able to predict the tumble center movement behind the spark plug in line with experimental observation.
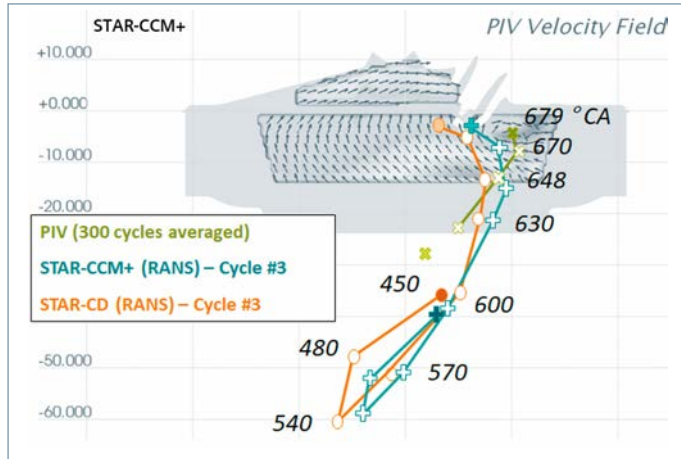

Figure 11: Tumble center traces as a function of crank angle overlaid with the PIV velocity field at 679° CA.

As noted, this is a crucial detail of the engine combustion stability and performance. Multicycle comparison proves that the velocity field and all the aforementioned flow features are only mildly changing in the Simcenter STAR-CCM+ solution after the second cycle.

Mesh sensitivity
The baseline mesh used in all previously described Simcenter STAR-CCM+ simulations was already comparably coarse (0.75 mm base size versus 0.4 mm base size for the STAR-CD solution) A mesh sensitivity was carried out to identify the limits of discretization sensitivity; see figure 12 and Table 3.

Table 3 – Meshes studied

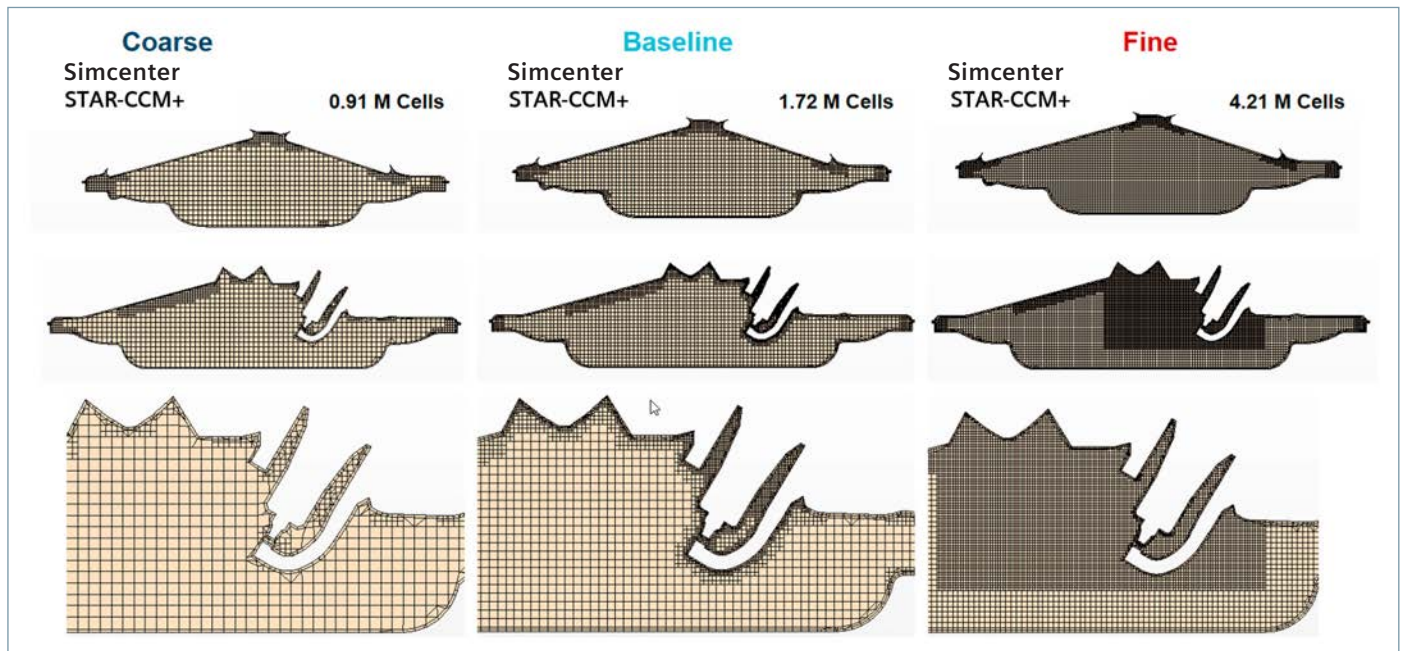| Resolution	coarse	baseline	fine
Base size (mm)	1.00	0.75	0.50
Spark plug refinement	no	Surface-based	Volume-based
Cell count @TDC (MM)	0.91	1.72	4.21
@BDC (MM)	1.47	3.10	8.69

Figure 12: Cylinder center section at top dead center of meshes studied in a grid resolution sensitivity study.

The study reveals that thermodynamic cylinder averaged properties (trapped mass, pressure, temperature) show a moderate mesh dependency – lower than code impact of STAR-CD versus. Simcenter STAR-CCM+. Moreover, multi-cycle impact is dominant over mesh resolution impact for these properties. Tumble and TKE show a more pronounced mesh impact; see figures 13 and 14.
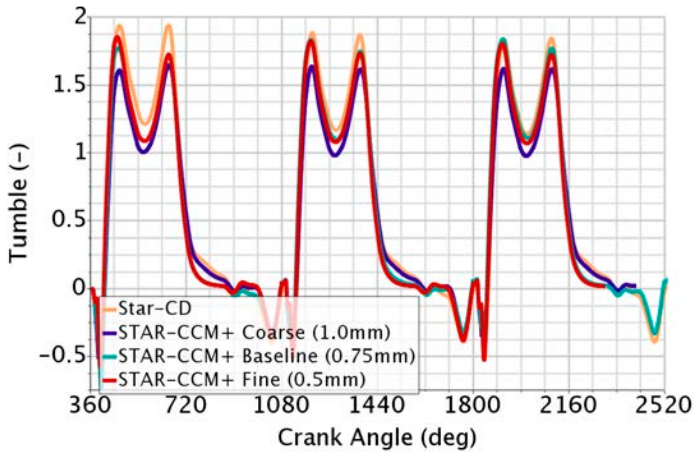

Figure 13: Mesh resolution sensitivity of transient tumble evolution.

The upstroke tumble evolution on the coarse mesh is similar to STAR-CD but different to fine and medium mesh (the latter very similar to each other – indicating mesh independency).
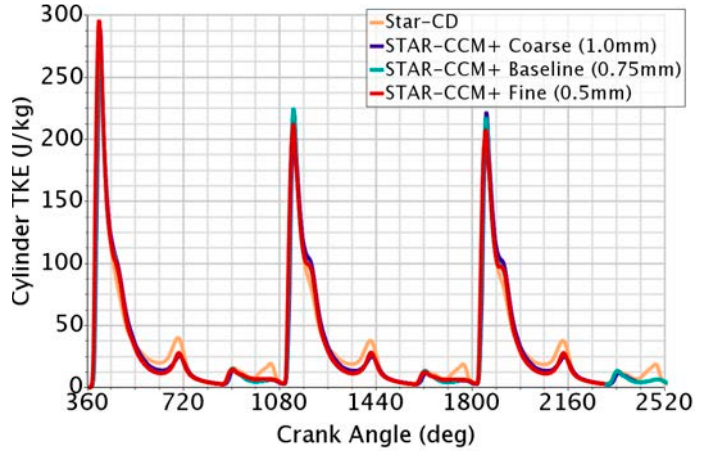

Figure 14: Mesh resolution sensitivity of transient TKE evolution.

TKE traces are very similar for all Simcenter STAR-CCM+ meshes but show notable differences to STAR-CD, especially for compression peak TKE. Here again, Simcenter STAR-CCM+ mesh dependency is lower than the code impact. This in return may be related to the different turbulence models employed in both codes (realizable k-epsilon versus standard k-epsilon) as will be discussed later.

Appendix C shows the velocity field in the central tumble plane for all meshes vs. PIV results: accordingly, the mesh impact on major features (intake jet, upward tumble, late compression upward flow) becomes negligible for mesh size lower than 0.75 mm. During upstroke, magnitudes of dominating flow features remain higher for mesh resolutions below 0.75 mm indicating a less diffusive solution and are thereby closer to PIV data.
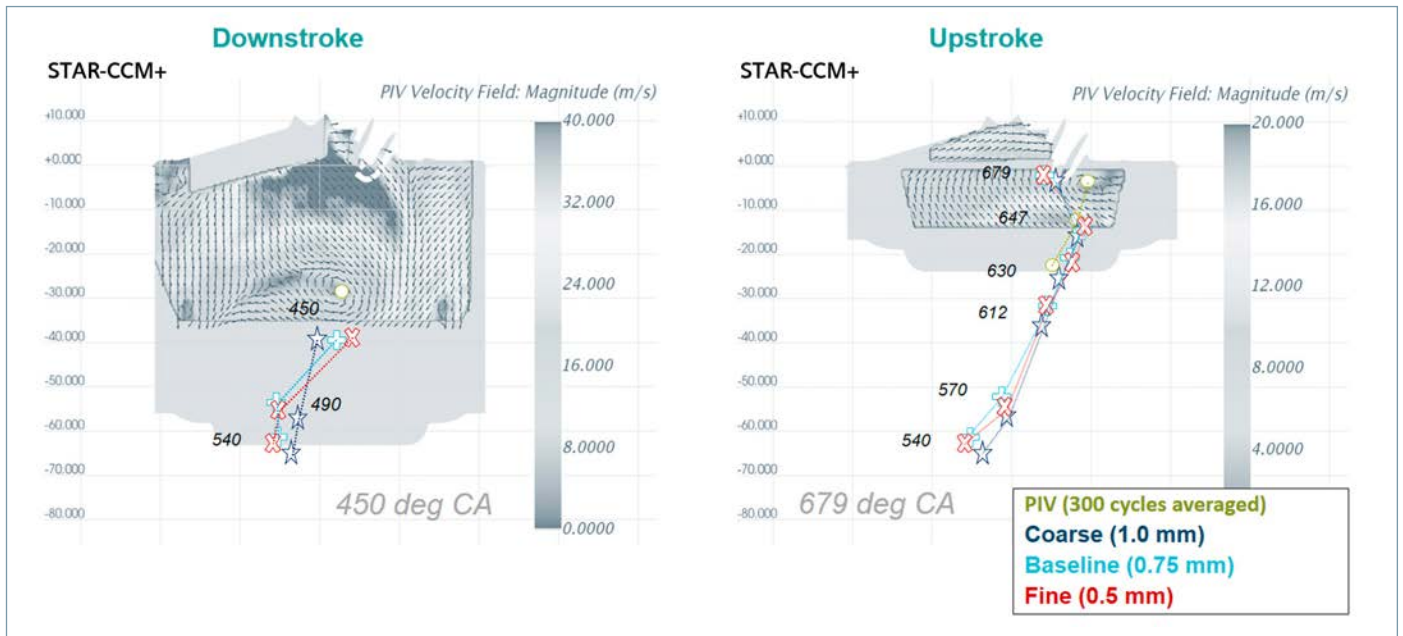
Figure 15: Mesh resolution sensitivity of transient tumble center traces.

The impact of mesh resolution on tumble traces during downstroke due to intake jet differences vanishes below 0.75 mm mesh size. Tumble traces become nearly mesh-insensitive during upstroke for all studies mesh resolutions as figure 10 proves.

Mesh resolution versus multi-cycle effect

Figure 16 summarizes the insights from the multi-cycle and mesh sensitivity study. It shows the total combined difference (RMS) of characteristic quantities (see legend of figure 7, top) from their respective reference value defined by their respective values in cycle 3 on the fine mesh.
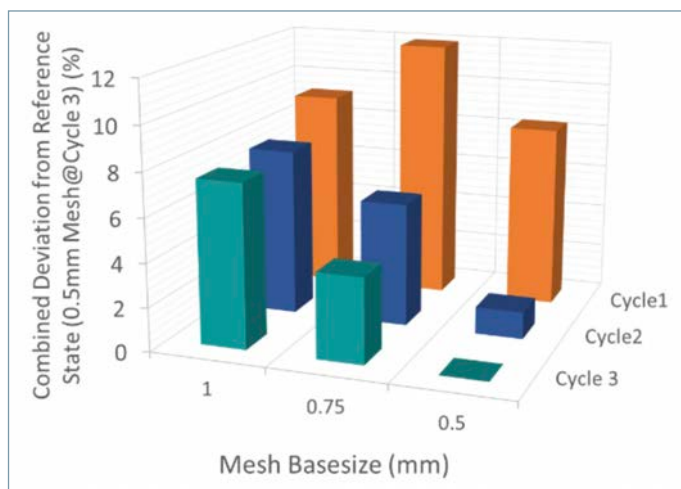

Figure 16: Quantification of grid resolution and cycle-by-cycle convergence.

The numbers prove that running a second cycle is strongly recommended while there is only a moderate benefit from a third cycle (regardless of the mesh resolution). Furthermore, second cycle impact dominates over mesh resolution impact between high and medium mesh resolutions. For the best compromise it is advisable to run two cycles on a medium resolution mesh (base size: 0.75 mm).

Turbulence model effect

The previous insights prove that global TKE evolution traces very are similar for all Simcenter STAR-CCM+ meshes but notable differences are visible in comparison to the STAR-CD solution, especially for compression peak TKE. For OEMs that typically have a legacy database of STAR-CD results it might therefore be of interest to achieve consistency as they migrate the CFD solver. Overall Simcenter STAR-CCM+ mesh dependency appears lower than code impact. However, up to now differences might still be triggered by different turbulence models employed in Simcenter STAR-CCM+ (realizable k-epsilon) and STAR-CD (standard k-epsilon) runs. To prove this hypothesis a check is carried out by switching to standard k-epsilon turbulence model in Simcenter STAR-CCM+ in line with STAR-CD settings using the Simcenter STAR-CCM+ baseline mesh configuration. It is important to emphasize that this study is not intended to judge if one turbulence model is superior to the other. It is predominantly about offering a consistent approach for STAR-CD legacy projects.

Note that the STAR-CD mesh naturally remains inconsistent with the STAR-ICE mesh.

The tumble evolution under the variation of the turbulence model in Simcenter STAR-CCM+ as compared to STAR-CD standard k-epsilon high Reynolds can be seen in figure 17.
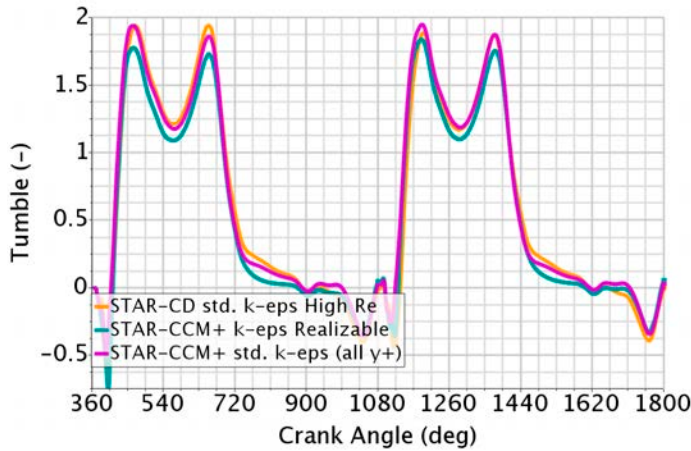

Figure 17: Tumble evolution under the variation of turbulence model and CFD solver.

The graphs prove that Simcenter STAR-CCM+ is approaching STAR-CD behavior if the standard k-epsilon model for most periods of the engine cycle is being used in both codes. Moreover, the turbulence model impact is dominating over the CFD code impact: for all periods but the early intake and exhaust, the respective Simcenter STAR-CCM+ results differ more under the variation of the turbulence model than the differences between STAR-CD and Simcenter STAR-CCM+ if the same turbulence model was being used in those. A similar observation can be made for the turbulent kinetic energy evolution; figure 18.
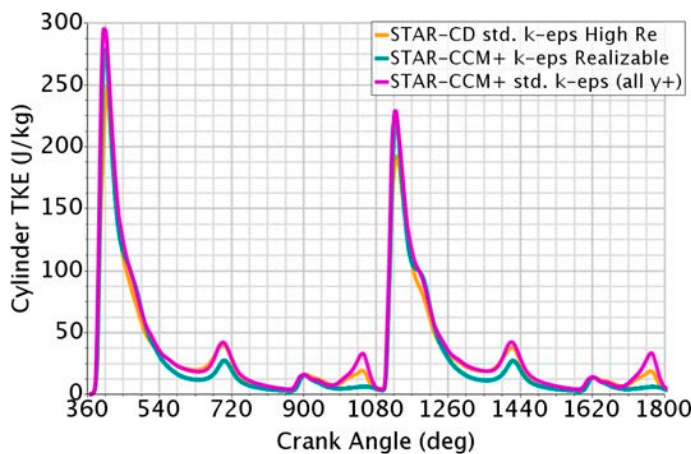

Figure 18: Turbulent kinetic energy evolution under the variation of turbulence model and CFD solver.

While the code impact is dominating turbulence model impact during early intake jet (downstroke) and exhaust phase, the two codes start to match in TKE with standard k-epsilon from compression stroke onwards to exhaust valve opening. Especially at ignition time STAR-CCM+ is perfectly matching STAR-CD behavior.

Figure 19 shows the respective tumble center trajectories under variation of the turbulence model in STAR-CCM+ compared to STAR-CD and PIV results. Generally, all setups capture the global trend motion in a similar manner.
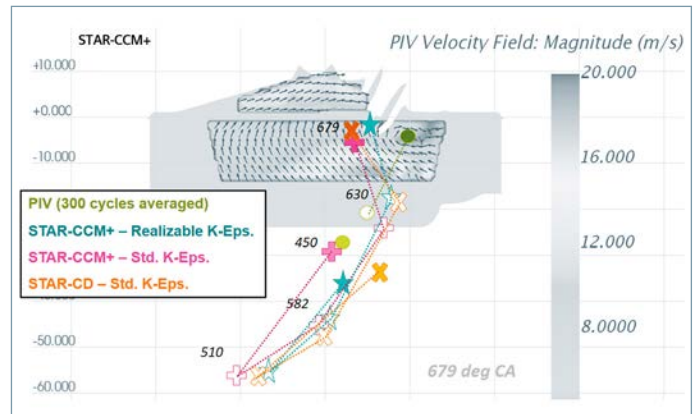

Figure 19: Turbulence model and CFD code sensitivity of transient tumble center traces.

However, in more detail, the very late compression phase is dominated by the turbulence model choice: here Simcenter STAR-CCM+ behaves similar to STAR-CD if both employ the standard k-epsilon model. In particular, the movement of the tumble center behind the spark plug as seen in the PIV is best captured by using the realizable k-epsilon model. This leads to the conclusion that the realizable k-epsilon turbulence model is a crucial element to achieve the superior tumble center location predictions from Simcenter STAR-CCM+, while a consistent solution between STAR-CD and Simcenter STAR-CCM+ can be achieved by using standard k-epsilon.
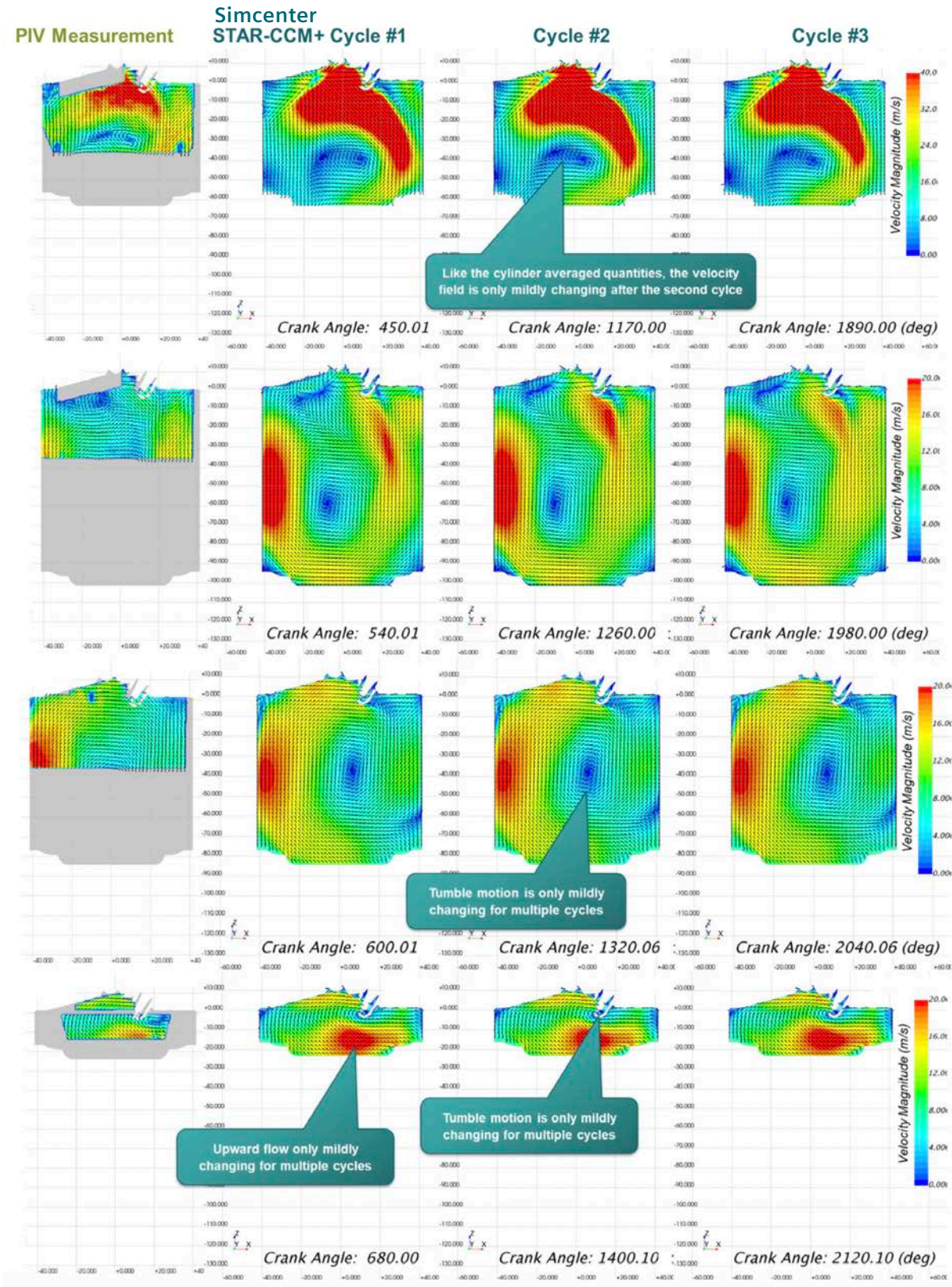
Appendix A: Baseline validation of the velocity field in the central tumble plane
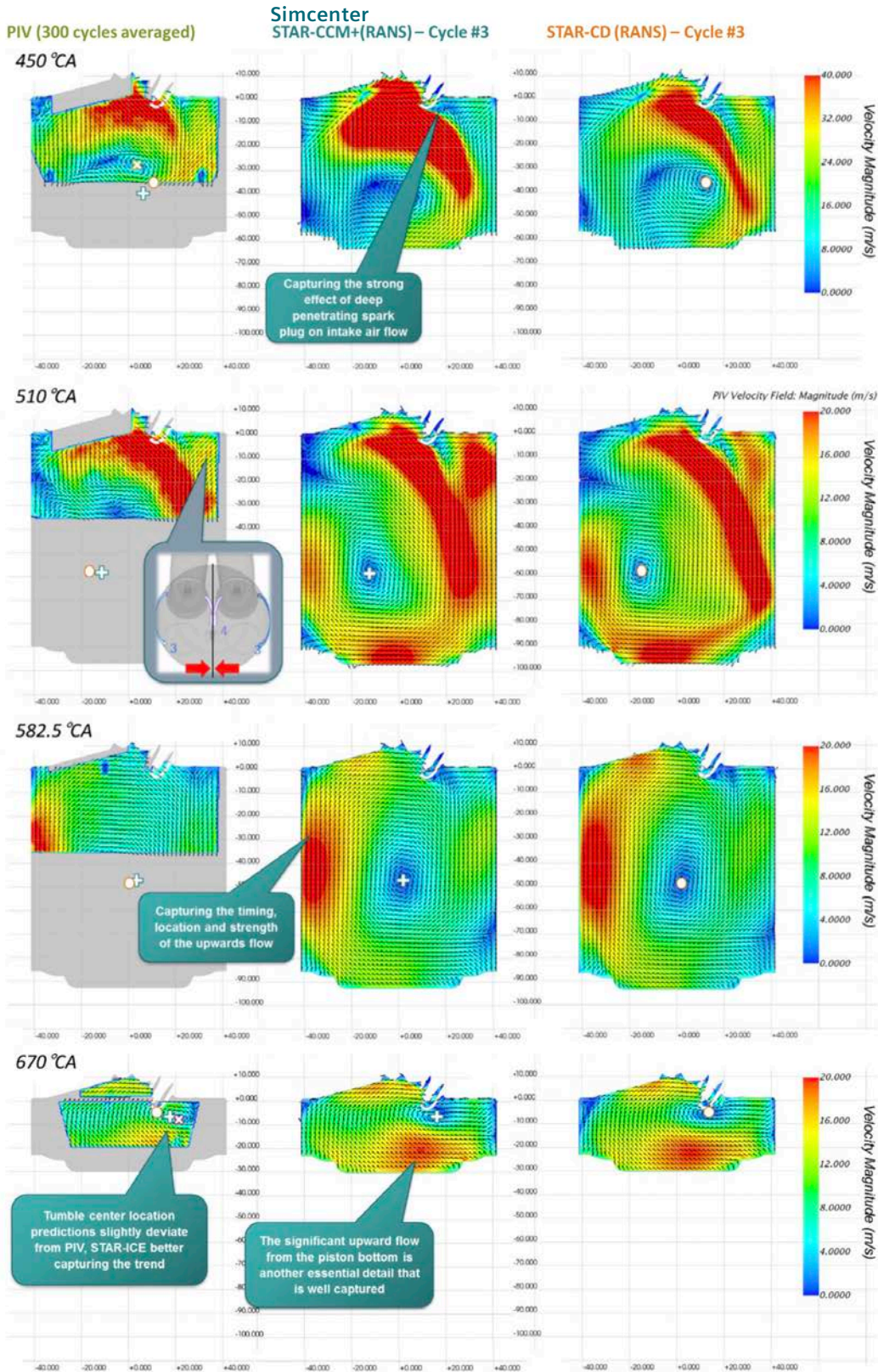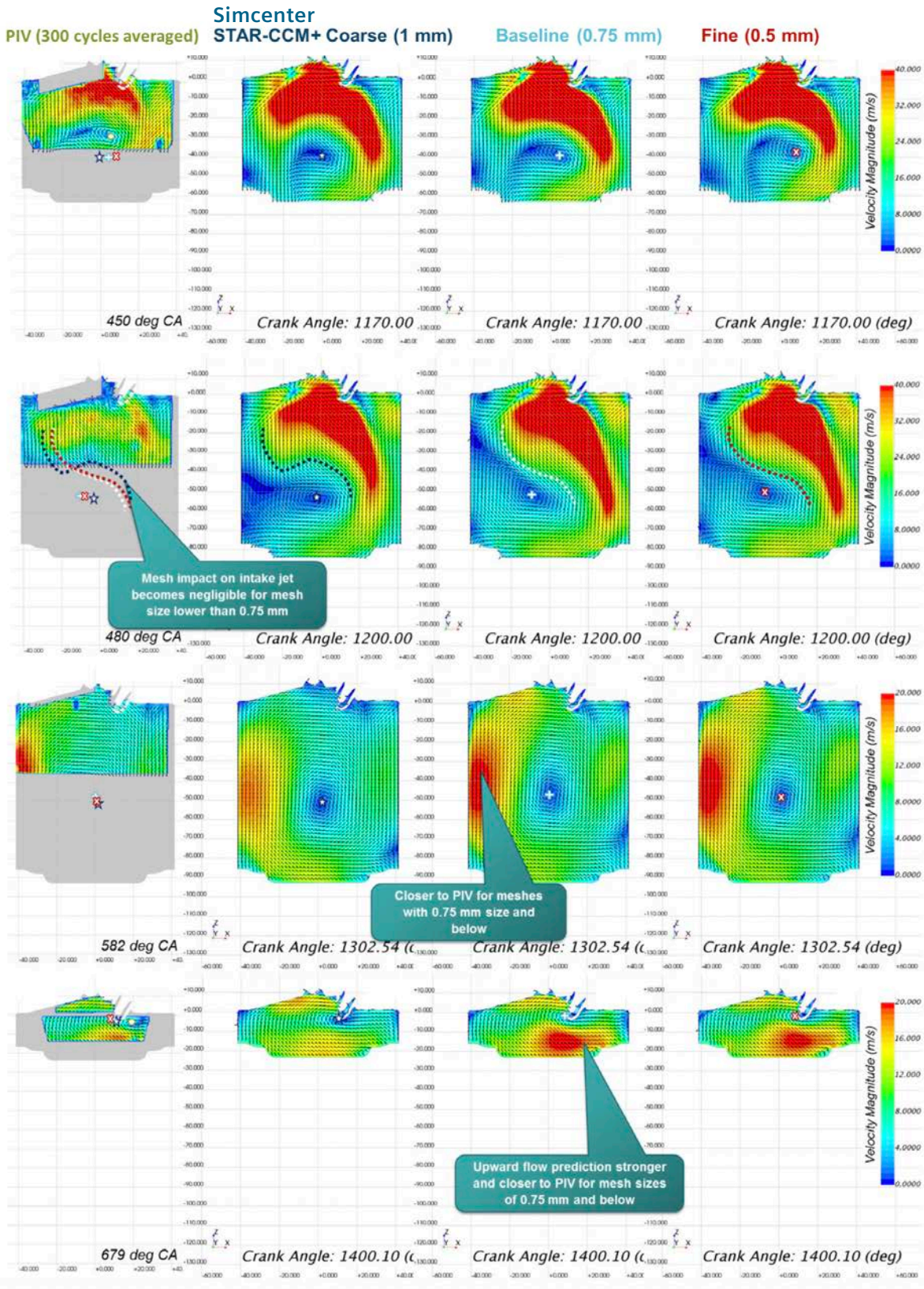
Appendix B: Multi-cycle impact on the velocity field in the central tumble plane
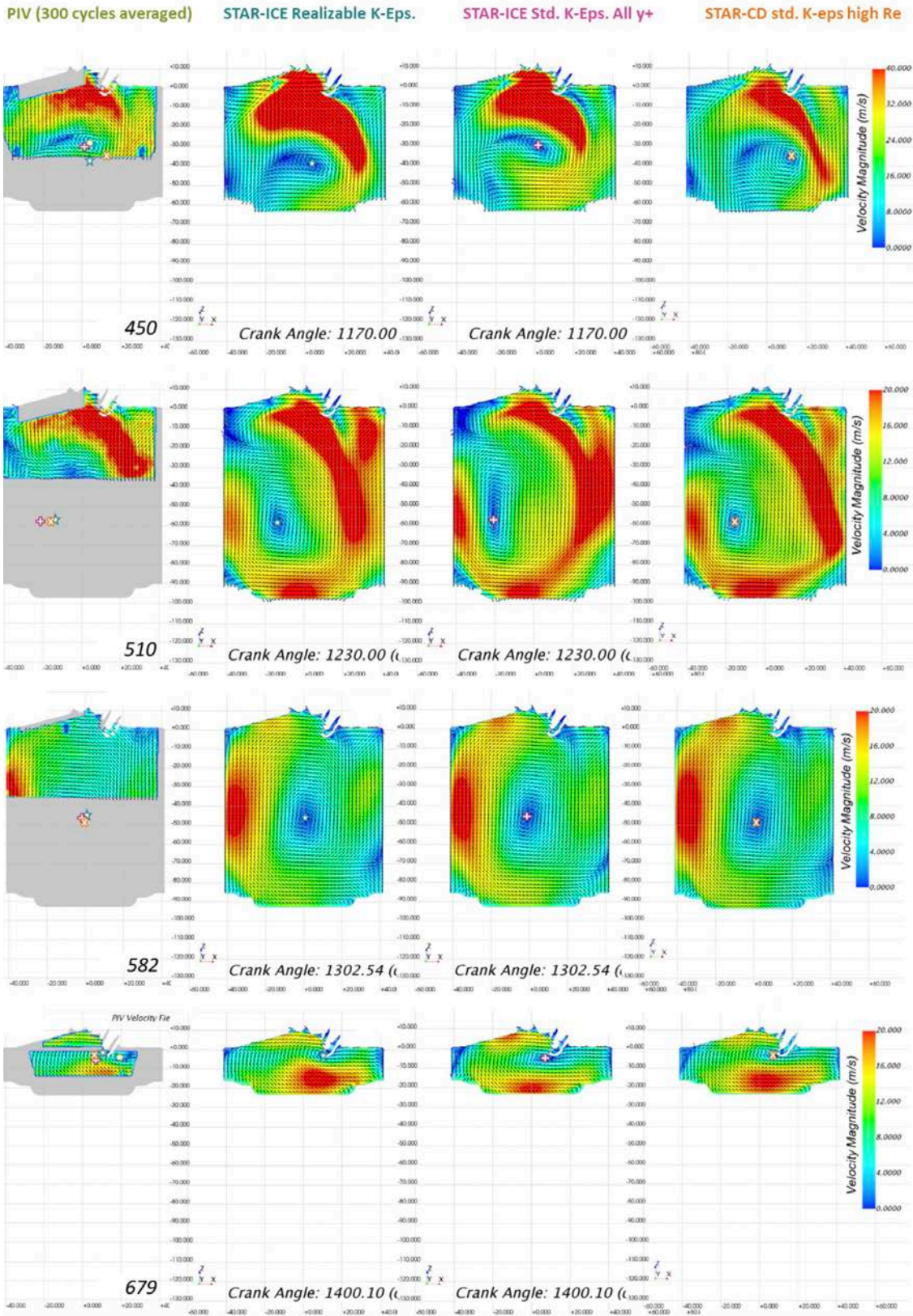
Appendix C: Mesh resolution impact on the velocity field in the central tumble plane

Appendix D: Turbulence model impact on the velocity field in the central tumble plane

Conclusion and outlook

The Simcenter STAR-CCM+ In-cylinder solution captures all major characteristic flow field features in line with PIV measurements. Global flow quantities predictions correspond to a STAR-CD reference solution. For turbulence evolution the two codes differ while a final judgement of the superior solution lacks availability of experimental insights. Tumble traces imply a more accurate prediction from Simcenter STAR-CCM+ if the realizable

k-epsilon turbulence model is employed. Cyclic convergence can be achieved within two cycles and mesh resolution impact becomes negligible below 0.75 mm base size. With the upcoming releases of Simcenter STAR-CCM+ the study will be extended to assessing spray injection and mixture preparation in a first step. It can be further extended to combustion and finally emissions simulation.

References

1. Gosman, A.D.: "State of the Art of Multi-Dimensional Modeling of Engine Reacting Flows", Oil & Gas Science and Technology – Rev. de l'IFP, Vol. 54 (1999), No. 2, pp. 149-159

2. Zellat, M., Abouri, D., Desoutter, G., Liang, Y., et al.: "State-of-the-Art of Modeling of Spark-Ignited Engine Reacting Flows: Differences and Similarities between Models Illustrated by Application and Validations," 26th International Multidimensional Engine Modeling User's Group Meeting, 2016.

3. Skeen, S., Manin, J., Pickett, L., Cenker, E. et al.: "A Progress Review on Soot Experiments and Modeling in the Engine Combustion Network (ECN)," SAE Technical Paper 2016-01-0734, 2016

4. D'Adamo, A., Breda, S., Fontanesi, S., Cantore, G.: "A RANS-Based CFD Model to Predict the Statistical Occurrence of Knock in Spark-Ignition Engines", SAE International Journal of Engines 9 (2016-01-0581), 618-630

5. Krüger,C., Schorr, J., Nicollet, F., Bode, J., Dreizler, A., Böhm, B.: "Cause-and-effect chain from flow and spray to heat release during lean gasoline combustion operation using conditional statistics," International Journal of Engine Research 2017, Vol. 18(1-2) 143–154, DOI: 10.1177/1468087416686721

6. Falfari, S., Forte, C., Brusiani, F., Bianchi, G. et al.: "Development of a 0D Model Starting from Different RANS CFD Tumble Flow Fields in Order to Predict the Turbulence Evolution at Ignition Timing," SAE Technical Paper 2014-32-0048, 2014, https://doi.org/10.4271/2014-32-0048

7. Jie, M., Kim, M., and Kim, W.: "The Effect of Tumble Flow on Engine Performance and Flame Propagation," SAE Technical Paper 931946, 1993, https://doi.org/10.4271/931946

8. Vent, G., Enderle, C., Merdes, N., Kreitmann F., Weller, R.: "The new 2.0l turbo engine from the Mercedes-Benz 4-cylinder engine family," Proceedings of the 21st Aachen Colloquium Automobile and Engine Technology 2012, 8-10 October 2012.

9. Jie, M., Kim, M., and Kim, W.: "The Effect of Tumble Flow on Engine Performance and Flame Propagation," SAE Technical Paper 931946, 1993, https://doi.org/10.4271/931946

10. Kang, K. and Baek, J.: "Tumble Flow and Turbulence Characteristics in a Small Four-Valve Engine," SAE Technical Paper 960265, 1996, https://doi.org/10.4271/960265

11. Shuliang, L., Yufeng, L., and Ming, L.: "Prediction of Tumble Speed in the Cylinder of the 4-Valve Spark Ignition Engines," SAE Technical Paper 2000-01-0247, 2000, https://doi.org/10.4271/2000-01-0247

Siemens Digital Industries Software

Headquarters
Granite Park One
5800 Granite Parkway
Suite 600
Plano, TX 75024
USA
+1 972 987 3000

Americas
Granite Park One
5800 Granite Parkway
Suite 600
Plano, TX 75024
USA
+1 314 264 8499

Europe
Stephenson House
Sir William Siemens Square
Frimley, Camberley
Surrey, GU16 8QD
+44 (0) 1276 413200

Asia-Pacific
Unit 901-902, 9/F
Tower B, Manulife Financial Centre
223-231 Wai Yip Street, Kwun Tong
Kowloon, Hong Kong
+852 2230 3333

About Siemens Digital Industries Software
Siemens Digital Industries Software is driving transformation to enable a digital enterprise where engineering, manufacturing and electronics design meet tomorrow. Our solutions help companies of all sizes create and leverage digital twins that provide organizations with new insights, opportunities and levels of automation to drive innovation. For more information on Siemens Digital Industries Software products and services, visit siemens.com/software or follow us on LinkedIn, Twitter, Facebook and Instagram. Siemens Digital Industries Software – Where today meets tomorrow.

siemens.com/software